

# Automated Stitching of Coral Reef Images and Extraction of Features for Damselfish Shoaling Behavior Analysis

Riza Rae A. Pineda  
*Department of Computer Science*  
*University of the Philippines*  
Quezon City, Philippines  
rapineda1@up.edu.ph

Kristofer E. delas Peñas  
*Department of Computer Science*  
*University of the Philippines*  
Quezon City, Philippines  
kedelaspenas@up.edu.ph

Dana P. Manogan  
*Marine Science Institute*  
*University of the Philippines*  
Quezon City, Philippines  
dmanogan@msi.upd.edu.ph

**Abstract**—Behavior analysis of animals involves the observation of intraspecific and interspecific interactions among various organisms in the environment. Collective behavior such as herding in farm animals, flocking of birds, and shoaling and schooling of fish provide information on its benefits on collective survival, fitness, reproductive patterns, group decision-making, and effects in animal epidemiology. In marine ethology, the investigation of behavioral patterns in schooling species can provide supplemental information in the planning and management of marine resources. Currently, damselfish species, although prevalent in tropical waters, have no adequate established base behavior information. This limits reef managers in efficiently planning for stress and disaster responses in protecting the reef. Visual marine data captured in the wild are scarce and prone to multiple scene variations, primarily caused by motion and changes in the natural environment. The gathered videos of damselfish by this research exhibit several scene distortions caused by erratic camera motions during acquisition. To effectively analyze shoaling behavior given the issues posed by capturing data in the wild, we propose a pre-processing system that utilizes color correction and image stitching techniques and extracts behavior features for manual analysis.

**Index Terms**—image stitching, marine images, fish behavior features

## I. INTRODUCTION

Behavioral data of fish provide salient information in the analysis of fish maturity, biological fitness, reproductive and seasonal cycles, and food chains [1]. This study may also provide appropriate behavioral models in the investigation of other vertebrates. Important fitness and survival benefits have been observed from the formation of mixed-species social groups among animals [2]. Many species of fish participate in group living such as schooling or shoaling for increased predator avoidance, better foraging and reproductive opportunities, and optimized energy use [3]–[8].

Damselfish species, which easily proliferate in reefs, have been observed to have detrimental effects to the recovery of coral reefs. This family of farmer fishes predominantly cultivate algal turfs and break juvenile corals to allow turf algae to grow [9]. However, collective information regarding how these species respond to their environment have yet to be

completely established. Reef managers are currently unable to obtain adequate information for the effective planning of reef restoration, rehabilitation, and sustainability projects.

At present, collecting behavior data in the wild is logistically and financially demanding, and physically exhausting. As events in the natural environment are inherently stochastic, sampling and capturing replicates are difficult and taxing. Currently, experts are only able to acquire snapshots of behaviors of the individuals since simulating a laboratory-like setup underwater is complex and often impractical.

Computer vision methods have been used to automate manual tasks in data preparation and processing. Corpuz et al. [10] proposed a rapid coral reef assessment system from towed camera arrays using mosaicking and an optimal seam search algorithms. With the capturing design of their method, translations and minimal rotations are expected from the collected images. Their method, as a result, may not perform well on data with high rotational variance.

Motivated by this technology and the need to establish more findings regarding damselfish species, we adapted the use of image correction and stitching techniques to provide more condensed details for damselfish behavior analysis. This research is in collaboration with an ongoing study on the shoaling behavior of damselfishes in coral reefs by the Marine Science Institute of the University of the Philippines. In the principal study [11], we analyze shoaling patterns to understand the internal organization of coral reef shoaling species. We support this goal by providing a visual dataset pre-processing tool that primarily produces trajectory maps and computes for behavior features which may then be utilized for further analysis.

Initially, we collected videos in two different reef sites in the Philippines. We then used an automatic white balancing algorithm to improve the color quality of the images. We labelled key points of objects and fish for each frame and submitted the frames for stitching, trajectory mapping, and behavior feature set extraction. Finally, we performed qualitative analysis and field expert validation on the resulting map and features.

R. R. Pineda is supported by a postgraduate scholarship from the Engineering Research and Development for Technology (ERDT), Philippines.

K. delas Peñas is supported by doctoral fellowships from the University of the Philippines and the Engineering Research and Development for Technology (ERDT), Philippines.

## II. METHODOLOGY

### A. Dataset

A total of 25 videos from two underwater sites in the Philippines, Batangas and Bolinao, with significantly different conditions were collected. Batangas is known to be a hotspot for diving activities due to its marine resource-rich location. This province in the Philippines is part of the Verde Island Passage, which has been declared as the center of marine shorefish biodiversity in the world [12]. Bolinao, on the other hand, is an established location for fisheries. The specific site selected from this province is a predominantly sandy location. Shown in Fig. 1 is a visual comparison of the two selected sites. The videos were captured using a single handheld GoPro Hero 4 camera at approximately 3 to 4 meters from the target individuals. Key points for each frame with reference to the first frame of the video sequence were manually labelled. Fish points corresponding to the head, center, and tail were individually annotated post color correction.

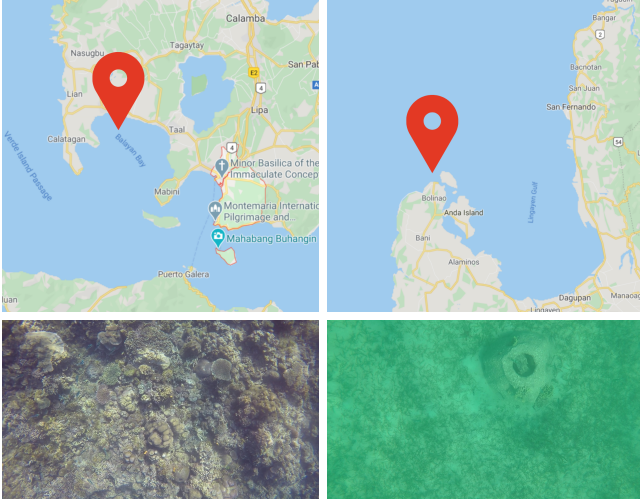


Fig. 1. Map locations (top row) of the two data sites, Batangas (left column) and Bolinao (right column), and sample raw image collected in each site (bottom row) displaying the difference in scene conditions

### B. Image Color Correction

Frames were sequentially extracted from the videos at a rate of 3 frames per second. Due to varying environmental conditions during the actual collection of the videos, the images captured had differing illuminations and noise. We initially employed an automatic white balancing algorithm designed by Lam [13] for color correction prior to stitching. In Lam's work, he proposed a quadratic mapping of intensities based on the gray world assumption and the Retinex theory for automatic white balancing [13].

1) *Gray World Assumption*: The underlying principle behind the gray world assumption is that the average of the negatives, which tends to be neutral, is biased towards dark regions of the image in film photography. For typical scenes, it is assumed that the average intensity of the red, green, and blue channels are equal [13]. This is given by,

$$R_{avg} = \frac{1}{MN} \sum_{x=1}^M \sum_{y=1}^N I_r(x, y) \quad (1)$$

$$G_{avg} = \frac{1}{MN} \sum_{x=1}^M \sum_{y=1}^N I_g(x, y) \quad (2)$$

$$B_{avg} = \frac{1}{MN} \sum_{x=1}^M \sum_{y=1}^N I_b(x, y) \quad (3)$$

where  $I$  is the  $M \times N$  image,  $r$  is the red channel,  $b$  is the blue channel,  $g$  is the green channel, and  $(x, y)$  are the 2D coordinates of each pixel.

Solely applying averaging does not generally produce good results. Therefore, the gain values  $\alpha$  and  $\beta$  of the red and blue channels, respectively, are computed for color correction [13]. The gain values are computed as,

$$\alpha = \frac{G_{avg}}{R_{avg}} \quad (4)$$

$$\beta = \frac{G_{avg}}{B_{avg}} \quad (5)$$

We then apply  $\alpha$  and  $\beta$  on the original image  $I$  for correction using the equations below:

$$\hat{I}_r(x, y) = \alpha I_r(x, y) \quad (6)$$

$$\hat{I}_b(x, y) = \beta I_b(x, y) \quad (7)$$

2) *Retinex Theory*: The Retinex theory states that the perceived white of humans is associated with the maximum cone signals of the eyes. To perform white balancing on images, the maximum values of the three color channels red, green, and blue must then be equalized. Similar to the gray world assumption, we use the red and blue channels and adjust the pixel values by multiplying the gain values to their respective channel [13].

3) *Automatic White Balance*: Combining the the gray world assumption and the retinex theory, the automatic white balance parameters  $\mu$  and  $v$  are given by:

$$\begin{bmatrix} \sum \sum I_r^2 & \sum \sum I_r \\ \max I_r^2 & \max I_r \end{bmatrix} \begin{bmatrix} \mu_r \\ v_r \end{bmatrix} = \begin{bmatrix} \sum \sum I_g \\ \max I_g \end{bmatrix} \quad (8)$$

$$\begin{bmatrix} \sum \sum I_b^2 & \sum \sum I_b \\ \max I_b^2 & \max I_b \end{bmatrix} \begin{bmatrix} \mu_b \\ v_b \end{bmatrix} = \begin{bmatrix} \sum \sum I_g \\ \max I_g \end{bmatrix} \quad (9)$$

where  $r$  and  $b$  pertain to the red and blue channel, respectively. Forming this as a system of linear equations with two unknowns,  $\mu$  and  $v$  for the two color channels can be solved by using Gaussian elimination [13]. Fig. 3 shows the original and color-corrected versions of a sample from each collected site. We also show the histogram of each image in Fig. 3 to provide more information on the differences in tonal distributions between the raw and corrected images.

The resulting images were then passed to the stitching module of the system to generate a reef map.

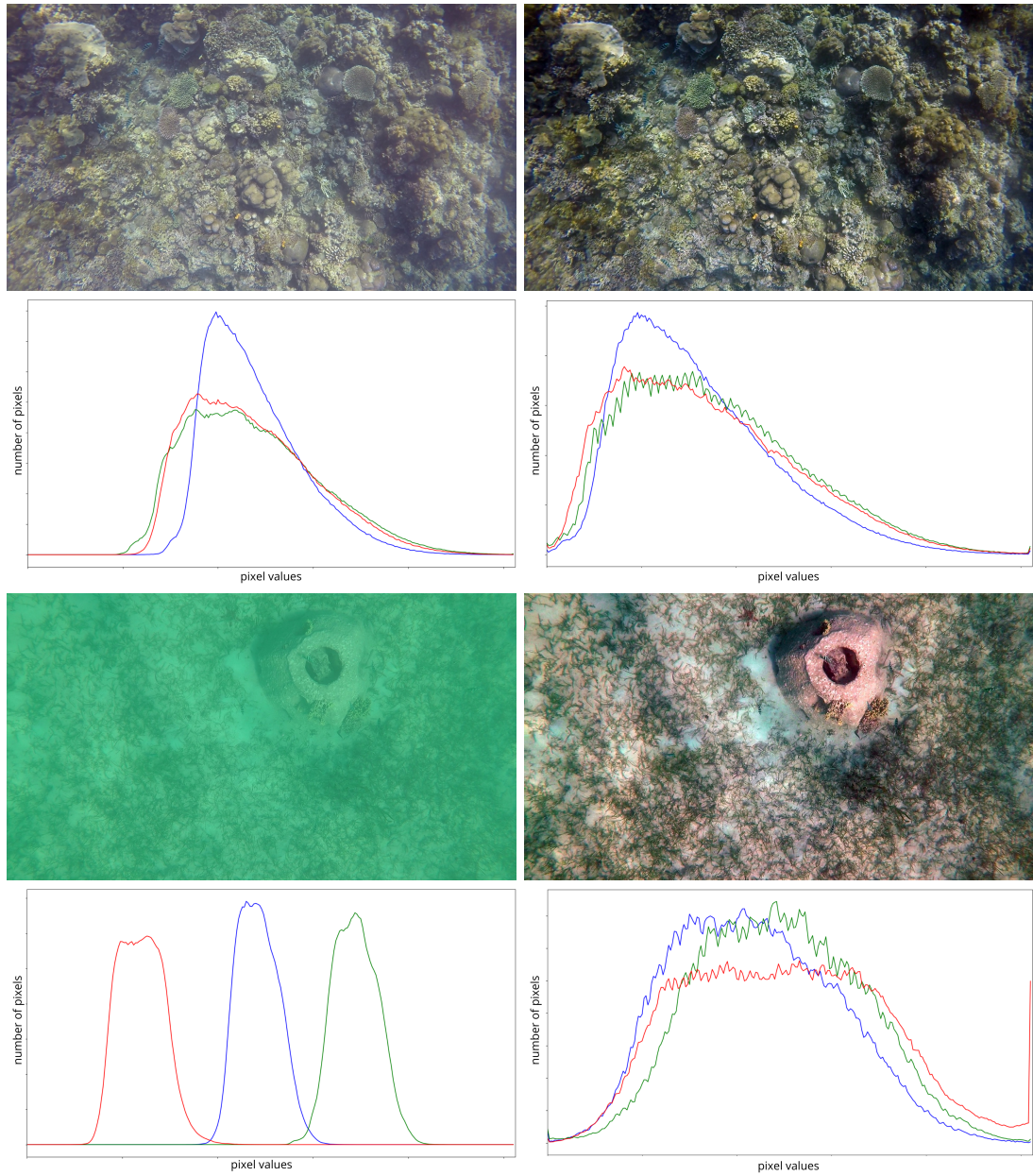


Fig. 2. Effect of applying the automatic white balancing algorithm of [13] in samples collected from the two data sites. The left column pertains to the raw information while the figures on the right column show the corrected information. For a densely noisy image, as in the lower left images, we observe a large disparity among the different channels. We perceive noticeable improvements in color after applying [13].

---

#### Algorithm 1 Image Stitching

---

- 1: **procedure** IMAGE STITCHING
  - 2:   Estimate the affine transformation matrix  $M$  of the current frame relative to the initial frame using RANSAC
  - 3:   Compute for the dimensions of the stitched map
  - 4:   Pad the images and their corresponding transformation matrices
  - 5:   Warp the current frame using the shifted transformation matrix
  - 6:   Combine the warped images and the initial frame
  - 7:   Apply morphological closing to remove black pixels between the overlay regions of succeeding frames
  - 8: **end procedure**
- 

#### C. Image Stitching

We performed image stitching through the steps defined in Algorithm 1. Once the sequence of frames were presented to the stitching function, transformation matrices were automatically computed using the Random Sampling Consensus (RANSAC) algorithm [14] for each succeeding frame relative to the initial frame.

The RANSAC [14] algorithm is a predictive model that generates candidate solutions using the minimum number of observations needed to estimate the underlying model parameters [14], [15]. This algorithm is described in Algorithm 2.

After the computation of the affine transformation matrices, the maximum and minimum dimensions from all the transformations were computed to determine the padding values. The initial frame was then padded and the transfor-



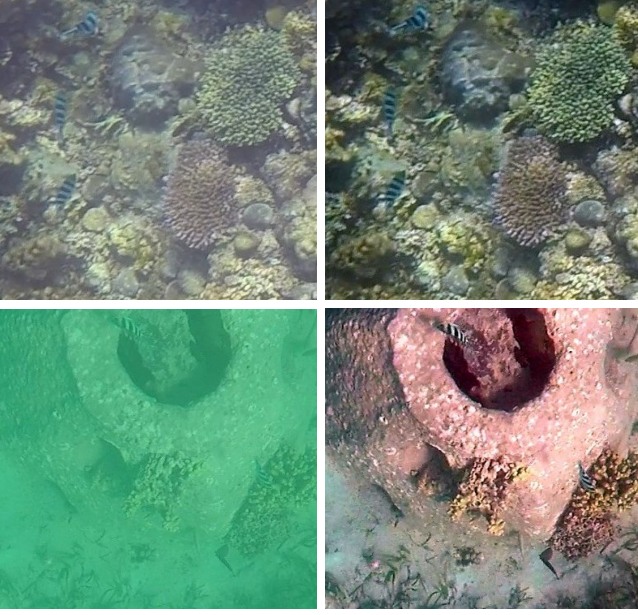


Fig. 3. A more detailed look on the effect of performing automatic white balancing on the collected images (raw images on the left; corrected images on the right). We see more recognizable objects richer in color as a consequence to applying [13].

---

**Algorithm 2** Random Sampling Consensus (RANSAC) [14], [15]

---

- 1: **procedure** RANSAC
  - 2:   Randomly select the minimum number of points required to determine the model parameters
  - 3:   Solve for the parameters of the model
  - 4:   Determine how many points from the set of all points fit with a predefined tolerance  $\epsilon$
  - 5:   If the fraction of the number of inliers over the total number points in the set exceeds a predefined threshold  $\tau$ , re-estimate the model parameters using all the identified inliers and terminate.
  - 6:   Otherwise, repeat steps 1 through 4 (maximum of N times)
  - 7: **end procedure**
- 

mation matrices of the succeeding images were shifted using the same padding parameters. Iteratively, each shifted affine transformation matrix was applied to its corresponding frame and superimposed on the current partial stitched map. As a result, we obtained an overall stitched map and smoothened the edges between the images by applying morphological closing. This method is a two-step procedure where the image is initially dilated and then eroded. Fig. 4 shows the difference between performing morphological closing on a subset of a sample stitched map.

The resulting image was then used to plot fish trajectories. Since fish points were manually labelled from the original orientation of each frame, a new set of corresponding points must be calculated for the stitched map. We performed this adjustment by applying the dot product of the shifted transformation matrix of the current frame to the original set points. This affine transformation method is given by

$$[x_{new}, y_{new}] = M_{shifted} \cdot [x_{orig}, y_{orig}, 1]^T \quad (10)$$



Fig. 4. Result of applying morphological closing on the stitched images. The top image contains black pixels as a result of warping and padding. We remove this by applying dilation and erosion on the whole image (bottom).

where  $x_{new}$  and  $y_{new}$  are the new fish coordinates in the transformed image,  $M_{shifted}$  is the translated  $2 \times 3$  transformation matrix of the current image, and  $x_{orig}$  and  $y_{orig}$  are the original fish coordinates.

The overall result of this section is a stitched map with plotted trajectories for each fish, shown in Fig. 5.

#### D. Shoaling Behavior Feature Extraction

After generating a trajectory segment for each individual in the video, we proceeded to the extraction of behavior features. The identified features are spatial distance travelled, overall displacement, average speed, estimated body length of each fish, and the distance, angle, and species of the head of each fish to the nearest fish.

1) *Total distance travelled*: The total distance travelled is given by the sum of all the Euclidean distances of each segment in the trajectory. This feature is measured in pixels.

2) *Overall displacement*: The overall displacement is the beeline distance from the start point to the end point.

3) *Average Speed*: The average speed, measured in pixels per second, is computed by dividing the total distance travelled by the total time travelled in seconds.

4) *Body Length*: Given three labelled points for each fish, head, center, and tail, the body length is computed as the sum of the lengths from the head to the center and the center to the tail. This feature is measured in pixels.

5) *Nearest Neighbor-based Features*: Rieucau et al. [16] identified two major features in the analysis of shoaling behavior in the wild. For each individual, he extracted the distance  $d$  to the nearest fish and the heading angle  $\theta$  with respect to the heading direction of the nearest fish. For each individual  $f_{curr}$  at each time frame, the distance  $d$  to the nearest fish  $f_{near}$  is the Euclidean distance and the heading angle  $\theta$  is computed with respect to its heading direction  $b$  and the heading direction of the nearest fish  $a$  using the inverse

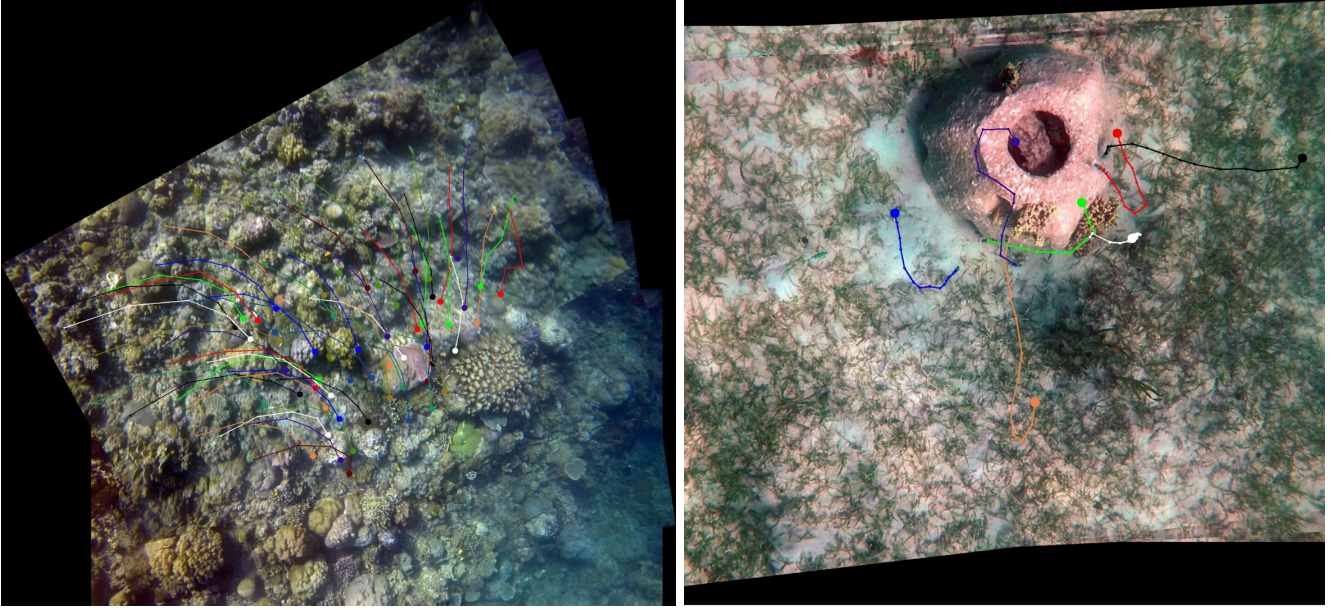


Fig. 5. Results of the stitching function. The top and bottom images are stitched maps generated from videos collected from the Batangas and Bolinao sites, respectively.

cosine function. Fig. 6 is a visualization of the computed parameters [16] for nearest neighbor-based features.

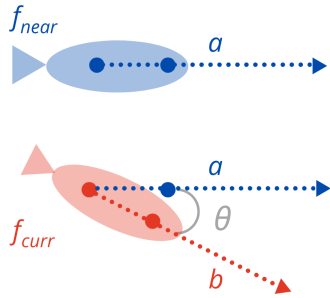


Fig. 6. Diagram for the nearest neighbor-based features. The blue circles correspond to the center and head points of  $f_{near}$ .  $a$  is the heading direction of  $f_{near}$ .  $b$  and the red dots are the heading direction, center point, and head point of  $f_{curr}$ , respectively.

### III. RESULTS AND DISCUSSION

1) *Automatic White Balancing*: Shown in Figures 2 and 3 are the significant improvements in the color quality of the images after performing automatic white balancing. The resulting images provide more contrasting information on the color of the damselfish individuals. Objects such as corals and grasses visually appear closer to their actual color than the raw data. In Fig. 2, the application of color correction significantly improved the color of both sample images. In the raw Bolinao videos, we can see frames with almost unrecognizable objects in the scene, especially in turbid waters. Inspecting further by looking into their histogram, we observe large disparities among the different color channels in these frames. Applying the method in [13], the disparity in the color distribution is reduced, resulting in frames with higher contrast. In these color-corrected frames, the color profile of the sea grasses are comparable to that of images in non-turbid waters.

2) *Image Stitching*: The stitched maps appear cohesive and near-seamless with negligible incorrect patches. As shown in Fig. 5, the trajectories displayed in the maps appear smooth and consistent despite multiple camera jitters and shaking during capture. This system is able to produce these results despite having only a single handheld camera as its capturing device. This makes this tool a viable alternative to more complex systems, such as those using rigs and stereo cameras, especially in instances where the travel load capacity for field works is limited.

The features generated appeared consistent with the visual information in the images and have been validated by our field expert.

The end-to-end automated process described in this research took only milliseconds in execution per video with 15 significant frames. This speed in processing videos demonstrates the potential of this work in high-throughput generation of shoaling behavioral features from marine data for further analysis of marine scientists.

### IV. CONCLUSION

We have shown in this paper a practical tool for pre-processing erratic visual data for marine scientists. Using our developed system, we remove the necessity of using specialized equipment other than a single underwater camera. This enhances the practicality and portability of the software most especially in conducting remote field work. This system hastens the data processing pipeline of marine scientists by producing summarized data without the need for manual evaluation of each video.

### V. FUTURE WORK

This research is in its early stages and multiple developments may be introduced to improve the tool. Full end to end automation can be introduced by improving the key point detection algorithm for stitching and using an automatic detector of fish.

## VI. AUTHORS

R. R. A. Pineda is currently a doctoral student majoring in information science and engineering in Nara Institute of Science and Technology, Japan. Her research interests lie in computer vision and animal behavior studies.

K. E. delas Penas is currently a doctoral student in the University of Oxford, United Kingdom, working on computer vision and biomedical image analysis.

D. P. Manogan is a graduating master's student from the Marine Science Institute of the University of the Philippines, Philippines. Her focus area is fish biology. She has extensive experience in conducting fish surveys and species identification.

- [16] G. Rieucan, J. Kiszka, J. Castillo, J. Mourier, K. Boswell, and M. Heithaus, "Using unmanned aerial vehicle (uav) surveys and image analysis in the study of large surface-associated marine species: a case study on reef sharks carcharhinus melanopterus shoaling behaviour," *Journal of Fish Biology*, vol. 93, 09 2018.

## REFERENCES

- [1] R. Fisher, Y.-H. Chen-Burger, D. Giordano, L. Hardman, and F.-P. Lin, *Fish4Knowledge: Collecting and Analyzing Massive Coral Reef Fish Video Data*, ser. Intelligent Systems Reference Library. Springer International Publishing, 2016.
- [2] E. Goodale, P. Ding, X. Liu, A. Martínez, X. Si, M. Walters, and S. K. Robinson, "The structure of mixed-species bird flocks, and their response to anthropogenic disturbance, with special reference to east asia," *Avian Research*, vol. 6, no. 1, p. 14, Aug 2015. [Online]. Available: <https://doi.org/10.1186/s40657-015-0023-0>
- [3] M. Abrahams and P. Colgan, "Risk of predation, hydrodynamic efficiency and their influence on school structure," *Environmental Biology of Fishes*, vol. 13, pp. 195–202, 07 1985.
- [4] J. Herskin and J. F. Steffensen, "Energy savings in sea bass swimming in a school: measurements of tail beat frequency and oxygen consumption at different swimming speeds," *Journal of Fish Biology*, vol. 53, no. 2, pp. 366–376, 1998. [Online]. Available: <https://onlinelibrary.wiley.com/doi/abs/10.1111/j.1095-8649.1998.tb00986.x>
- [5] S. Marras, S. S. Killen, J. Lindström, D. J. McKenzie, J. F. Steffensen, and P. Domenici, "Fish swimming in schools save energy regardless of their spatial position," *Behavioral Ecology and Sociobiology*, vol. 69, no. 2, pp. 219–226, Feb 2015. [Online]. Available: <https://doi.org/10.1007/s00265-014-1834-4>
- [6] D. WEIHS, "Hydromechanics of fish schooling," *Nature*, vol. 241, no. 5387, pp. 290–291, Jan 1973. [Online]. Available: <https://doi.org/10.1038/241290a0>
- [7] J. Snekser, N. Ruhl, K. Bauer, and S. McRobert, "The influence of sex and phenotype on shoaling decisions in zebrafish," *International journal of comparative psychology / ISCP; sponsored by the International Society for Comparative Psychology and the University of Calabria*, vol. 23, pp. 70–81, 01 2010.
- [8] L. E. Nadler, S. S. Killen, P. Domenici, and M. I. McCormick, "Role of water flow regime in the swimming behaviour and escape performance of a schooling fish," *Biology Open*, vol. 7, no. 10, 2018. [Online]. Available: <https://bio.biologists.org/content/7/10/bio031997>
- [9] S. A. Schopmeyer and D. Lirman, "Occupation dynamics and impacts of damselfish territoriality on recovering populations of the threatened staghorn coral, *acropora cervicornis*," Nov 215AD. [Online]. Available: <https://journals.plos.org/plosone/article?id=10.1371/journal.pone.0141302>
- [10] F. J. Corpuz, P. Naval, E. Capili, J. Jauod, R. J. Judilla, and M. Soriano, "Coral reef mosaicking using teardrop and fast image labeling," in *2012 Oceans - Yeosu*, 2012, pp. 1–6.
- [11] D. Manogan, P. Cabaitan, K. Stiefel, R. R. Pineda, and P. J. Naval, "Tracking damselfish shoals," 2020, unpublished.
- [12] K. Carpenter and V. Springer, "The center of the center of marine shore fish biodiversity: The philippine islands," *Environmental Biology of Fishes*, vol. 72, pp. 467–480, 04 2005.
- [13] E. Lam, "Combining gray world and retinex theory for automatic white balance in digital photography," 07 2005, pp. 134 – 139.
- [14] M. A. Fischler and R. C. Bolles, "Random sample consensus: A paradigm for model fitting with applications to image analysis and automated cartography," *Commun. ACM*, vol. 24, no. 6, p. 381395, Jun. 1981. [Online]. Available: <https://doi.org/10.1145/358669.358692>
- [15] K. G. Derpanis, "Overview of the ransac algorithm," May 2010. [Online]. Available: [http://www.cse.yorku.ca/~kosta/CompVis\\_Notes/ransac.pdf](http://www.cse.yorku.ca/~kosta/CompVis_Notes/ransac.pdf)